Bioprocess Biosyst Eng (2009) 32:531–536
DOI 10.1007/s00449-008-0273-x

ORIGINAL PAPER

Disposable superoxide anion biosensor based on superoxide dismutase entrapped in silica sol–gel matrix at gold nanoparticles modified ITO electrode

Yuan Wang · Ying Wu · Jianwen Wang · Junwei Di

Received: 6 October 2008 / Accepted: 10 October 2008 / Published online: 4 November 2008

Abstract A novel disposable biosensor based on direct electron transfer of superoxide dismutase (SOD) was fabricated for the determination of superoxide anion. The biosensor was constructed by electrodeposition of gold nanoparticles (GNPs) on the indium tin oxide (ITO) electrode and then immobilization of SOD in silica sol–gel (SG) network in the presence of cysteine on GNPs/ITO modified electrode surface. The distribution of GNPs on ITO electrode surface was examined by scanning electron microscopy (SEM). The immobilized SOD exhibited high catalytical activity towards superoxide anion. Parameters affecting the performance of the biosensor were also investigated. A linear calibration curve was obtained over the range from 0.08 to 0.64 μM with a correlation coefficient of 0.9937. The resulted biosensors were demonstrated to possess striking analytical properties for superoxide anion determination, such as high sensitivity, good accuracy, and long-term stability. It provides a promising platform for the fabrication of disposable biosensors.

Keywords Biosensor · Gold nanoparticles · Sol–gel · Superoxide dismutase · Superoxide anion

Introduction

Superoxide anion ($O_2^{\cdot -}$) is one of the most abundant radicals produced in biological systems. It is a transient reduction product of molecular oxygen (O_2) in mitochondria or in the presence of certain kinds of antioxidant (such as ascorbic acid, α-tocopherol, catecholamines, etc.) and antioxidant enzymes (such as nitric oxide synthase and NAD(P)H peroxidase). Superoxide anion is mostly considered to be toxic, because biological systems can convert it into other more reactive species, such as alkoxyl ($RO^{\cdot}$), hydroxyl radical ($HO^{\cdot}$) and peroxynitrite (ONOO–). With an increase of superoxide anion, it directly/indirectly results in an inhibition of cell growth, mutagenesis, and cell death [1–6].

Therefore, the quantitative determination of superoxide anion concentrations and the beneficial effects of antioxidant compounds are of great interest. The methods commonly used to determine superoxide anion are electron spin resonance [7], chromatograph [8, 9], chemiluminescence [10], fluorescence [11], and spectrophotometry [12].

Recently, electrochemical methods based on protein chemistry would offer a direct, real time measurement in biological systems with minimal disturbance to the sample under investigation [13]. Superoxide dismutase (SOD), which was believed to be the only way to metabolize the superoxide anion [2], is mostly used for this purpose [14, 15]. Especially, the direct electrochemistry of SOD between enzyme and electrode surface has been realized [16, 17]. The direct electron transfer of SOD could be efficiently facilitated by self-assembled monolayer (SAM) of thiol confined on gold electrodes, and that a combination of such a well-promoted electron transfer properties with the highly specific catalytic activity of the SOD towards superoxide anion dismutation substantially make it possible to fabricate SOD-based third-generation electrochemical biosensor for superoxide anion. Gold nanoparticles (GNPs) as a base for the immobilization of SOD have also been used to realize direct electron transfer of SOD duo to their excellent biological compatibility and large surface area [18–20]. With the benefits of the advantage of GNPs, self-assembly and

Y. Wang · Y. Wu · J. Wang · J. Di (✉)
Department of Chemistry, Suzhou University,
215123 Suzhou, Jiangsu, People's Republic of China
e-mail: djw@suda.edu.cn

the microenvironment of SG network structure, we also developed a high sensitive and long-time stable superoxide anion biosensor based on embedding SOD and GNPs in silica sol–gel (SG) network in the presence of cysteine [21].

However, the utility of an enzyme-based electrode may be limited by the gradual fouling of its surface and/or loss of enzyme activity. Such a problem can be minimized with the use of disposable electrodes. Low cost of construction and possibility of large-scale production of these devices are some basic characteristics for an electrode to be considered as disposable.

In the present work, we would like to present a novel strategy to fabricate a disposable superoxide anion biosensor, which is based on SOD entrapped in silica SG matrix at GNPs electrodeposited on indium tin oxide (ITO) film coated glass. ITO electrode is used as substrate due to its low cost and prominent characteristics, such as high electrical conductivity, wide electrochemical working window, stable electrochemical and physical properties, and excellent substrate adhesion. Electrodeposition and SG techniques are possible for large-area and large-scale production. Therefore, the present strategy is promising for construction of disposable superoxide anion biosensors with high selectivity and sensitivity for real time monitoring of superoxide anion concentration and the characterization of the influence of antioxidants on their concentration.

Experimental

Chemicals and apparatus

SOD 3,200 U mg^{-1} (EC 1.15.11) and $KAu(CN)_2$ were obtained from Suzhou University (Suzhou, China). Xanthine oxidase (XOD) was purchased from Sigma Chemical Co. (St. Louis, MO). L-Cysteine (Cys) was purchased from Guoyao Chemical Regent Co., Ltd (Shanghai, Chain). Aqueous solution of Cys was freshly prepared. A polyvinyl alcohol (PVA) (average degree of polymerization was 2,400–2,500, Shanghai Chemical Reagent Plant imported from Japan) stock solution was prepared by dissolving it in 100 mL water under heating to near boiling. 0.05 mol L^{-1} phosphate buffer solution (PBS) was prepared by NaH_2PO_4 and Na_2HPO_4. All other chemicals were of analytical grade and used as received without further purification. All aqueous solutions were prepared in doubly distilled water.

Electrochemical measurements were performed with a conventional three-electrode electrochemical cell using a CHI 830B electrochemical analyzer (CH Instruments, Shanghai Chenhua Co.). A platinum wire auxiliary electrode and the saturated calomel reference electrode were used. The bare ITO electrode and the modified ITO electrode were used as the working electrode. The electrolyte was deoxygenated by bubbling nitrogen for at least 10 min, and a nitrogen atmosphere was kept over the solution during measurements. The adsorption spectrum was obtained with UV-Vis 2810 instrument (Hitachi, Japan) against bare ITO glass as reference in the air. Scanning electron microscopy (SEM) was run with an S-4700 scanning electron microanalyzer (Hitachi, Japan).

Preparation of SOD–Cys–SG/GNPs/ITO electrodes

Silica colloidal sol was prepared as described previously [16]. $Na_2SiO_3 \cdot 9H_2O$ was stored at 110 °C for 12 h. After cooling down, it was adjusted to specific gravity 1.38 with 3 M HCl. Then the silica sol was obtained by ion-exchange method from the diluted (addition of same volume water) solution. Finally, the stock silica sol was prepared by addition of 1/10 volume of 0.1% PVA.

A sheet of ITO glass was ultrasonicated in NH_3–H_2O (1:3), ethanol, and distilled water for 5 min consequently. After cleaning, the glass sheet was immersed into the solution of 0.1 mM $KAu(CN)_2$ in 0.05 M phosphate buffer solution (pH 7.5). (*Caution! Cyanide complex is virulent and should be handled with extreme care.)* The electrodeposition was performed by cyclic voltammetric mode at 50 ± 2 °C. The potential range of −0.2 to −1.3 V was applied for 20 cycles at 50 mV s^{-1}. After rinsing with water, the GNPs/ITO modified electrode (working area 0.6 × 0.6 cm^2) was dipped in the mixed solution containing in each milliliter 0.30 mL of silica sol, 0.25 mL of 1,000 U mL^{-1} SOD, and 0.15 mL of 0.01 M cysteine. Then, the electrode was kept for 3 h at room temperature under nitrogen atmosphere. The enzyme electrodes were stored at 4 °C in a dry state when not in use.

For comparison, the SOD/Cys/GNPs/ITO electrode was prepared by soaking the freshly prepared GNPs/ITO modified electrode in 1 mM Cys aqueous solution (N_2-saturated) for 4 h at room temperature. After the electrode was thoroughly rinsed with water to remove physically adsorbed Cys, the electrode was incubated in 1,000 U mL^{-1} SOD for 6 h to fabricate the enzyme electrode. The SOD/GNPs/ITO electrode was fabricated by soaking the GNPs/ITO modified electrode directly in 1,000 U mL^{-1} SOD for 6 h and rinsed with water.

Results and discussion

SEM characterization of GNPs/ITO modified electrode

Figure 1 shows a typical SEM image of an ITO electrode surface after GNPs modification with direct electrochemical

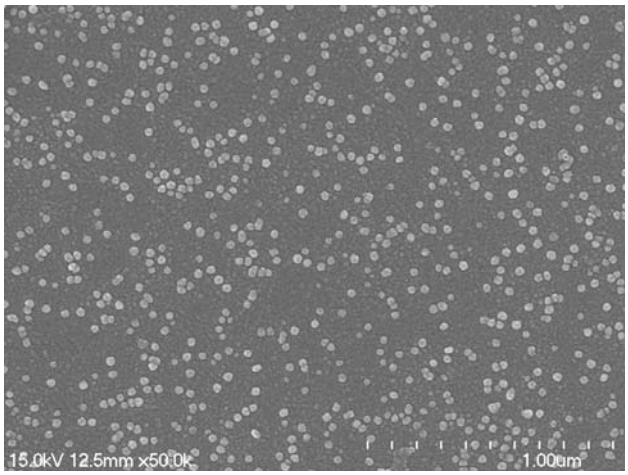

Fig. 1 SEM image of a GNPs/ITO electrode surface

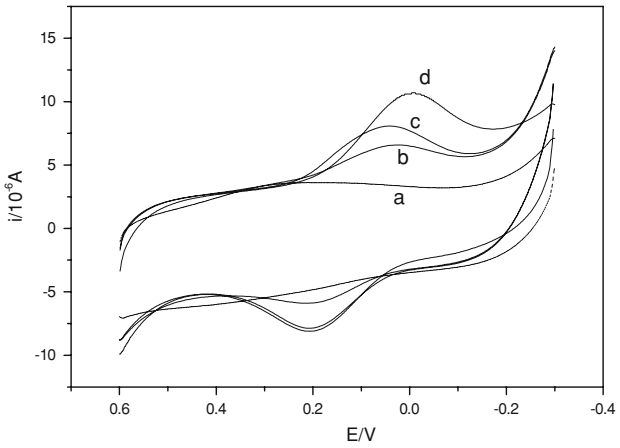

Fig. 2 Cyclic voltammograms obtained at GNPs/ITO electrode (**a**), SOD/GNPs/ITO electrode (**b**), SOD/Cys/GNPs/ITO electrode (**c**) and SOD–Cys–SG/GNPs/ITO electrode (**d**) in 0.05 M PBS (pH 6.8) at scan rate of 0.1 V s^{-1}

deposition. It can be seen that many quasi-spherical GNPs are deposited on the ITO electrode surface with a quite symmetric distribution. The average diameter of these quasi-spherical nanoparticles is about 28 nm. The cause may be that the growth of GNPs is well controlled by the slowly increasing potential rate and the very tiny particles are dissolved in the anodic process. The average size of GNPs is much smaller than that of the report [22], which obtain the average size of GNPs more than 100 nm. These small GNPs almost uniformly distributed on the ITO electrode surface are very useful for fabrication of enzyme-based biosensors, because each GNP can be used to immobilize SOD and served as sensing unit for determination of superoxide anion with high sensitivity.

Electrochemical properties of SOD–Cys–SG/GNPs/ITO modified electrode

The rate of the direct electron transfer between the active of SOD and the electrode surface is very slow, because the active site of SOD molecular is deeply embedded. The direct electron transfer of SOD could be efficiently facilitated by self-assembled monolayer of thiols and disulfides confined on gold electrodes [23]. Figure 2 shows cyclic voltammograms of GNPs/ITO, SOD/GNPs/ITO, SOD/Cys/GNPs/ITO, SOD–Cys–SG/GNPs/ITO electrode in 0.05 mV PBS at 0.1 V s^{-1}. No peak was observed at GNPs/ITO electrode (Fig. 2a). SOD–Cys–SG/GNPs/ITO electrode exhibited a well-defined redox wave with a formal potential (estimated as the average of cathodic and anodic peak potential) about 100 mV (vs. SCE) (Fig. 2d). The direct electron transfer between SOD and the electrode surface can be achieved by the favored orientation of SOD molecular and/or the conducting channels of GNPs. On the other hand, the cyclic voltammogram of SOD–Cys–SG/GNPs/ITO electrode was similar to that of SOD/GNPs/ITO (Fig. 2b) and SOD/Cys/GNPs/ITO electrode (Fig. 2c). Moreover, the peak current was markedly higher than that of SOD/GNPs/ITO or SOD/Cys/GNPs/ITO electrode after obtaining a steady-state cyclic voltammogram. The cause may be that SOD can firmly entrap inside the SG network onto the cysteine-modified GNPs deposited on ITO electrode.

The peak-to-peak separation between the cathodic and anodic peak potential is 210 mV at scan rate 100 mV s^{-1}. This suggests that the electrochemical process of SOD immobilized in SG network on GNPs/ITO modified electrode is quasi-reversible. At low scan rate ($\leq$0.5 V s^{-1}), the cathodic and anodic peak currents were direct proportional to the scan rate (v). The regression equations are: i_{pc} (μA) = 1.90 + 48.9v (V s^{-1}) with correlation coefficient 0.9951 and i_{pa} (μA) = −1.65 − 41.0v (V s^{-1}) with correlation coefficient 0.9943. It indicated that the electrode reaction is typical of surface-controlled quasi-reversible process.

Optimization of the enzyme electrode preparation

The effect of electrodeposition potential on the response of cyclic voltammetry at SOD–Cys–SG/GNPs/ITO electrode is investigated when the positive applied potential is fixed at −0.2 V (Fig. 3). The cathodic response rapidly increases with decreasing negatively applied voltage from −1.0 to −1.3 V and reaches plateau after −1.3 V. Inset of Fig. 3 illustrates the absorption spectra of GNP/ITO substrates against the bare ITO glass in the air at different negative applied potentials. The plasmonic absorptivity of GNPs increases with decreasing negatively applied voltage, which indicates the increase of the GNP density on ITO electrode surface. The GNPs/ITO modified electrode is red when the

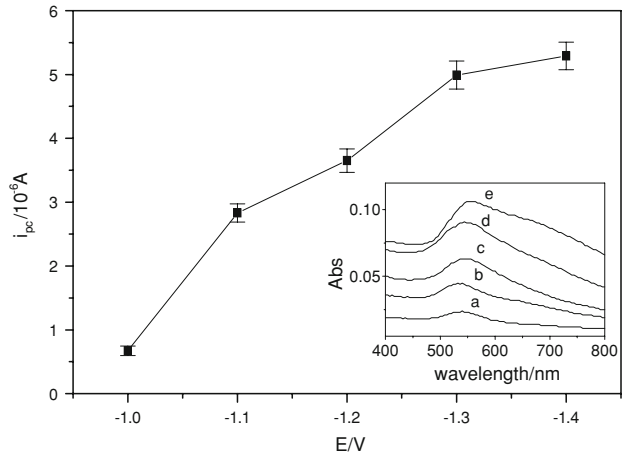

Fig. 3 Effect of the negative applied potential on cathodic peak current of SOD–Cys–SG/GNPs/ITO electrode in 0.05 M PBS at 100 mV s^{-1}. *Inset* the absorption curve of GNPs/ITO substrate. The negative applied potential: *a* −1.0, *b* −1.1, *c* −1.2, *d* −1.3, *e* −1.4 V

negative applied potential is in the range of −1.0 to −1.3 V. However, the GNPs/ITO modified electrode became red-blue color when the negative applied voltage was −1.4 V. This suggests that some GNPs were aggregation on the ITO electrode surface; therefore, we chose the electrodeposition voltage from −0.2 to −1.3 V.

The dependence of the electrodeposition cycles in the enzyme electrode preparation is shown in Fig. 4. The cathodic peak current increases gradually with increasing cycles of GNP deposition, and the plateau appeared after the electrodeposition was over 20 cycles. The absorptivity also increases with increasing cycles of deposition (inset of Fig. 4). Furthermore, when the electrodeposition is 30 cycles, the GNPs on ITO electrode also turn out red-blue

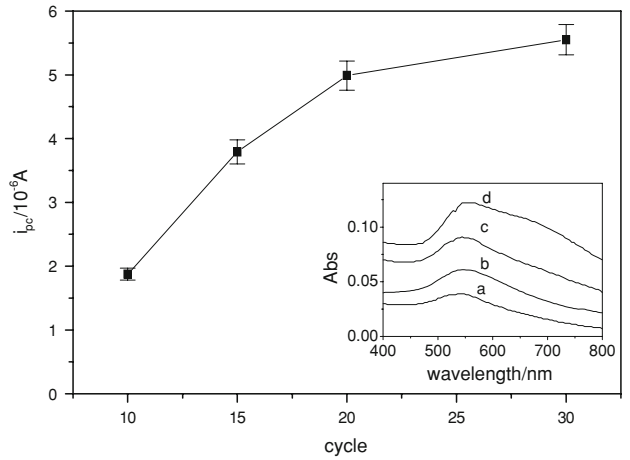

Fig. 4 Effect of electrodeposition cycles on cathodic peak current of SOD–Cys–SG/GNPs/ITO electrode in 0.05 M PBS at 100 mV s^{-1}. *Inset* the absorption curve of GNPs/ITO substrate. The electrodeposition cycles: *a* 10, *b* 15, *c* 20, *d* 30 cycles

color, which indicates the aggregation of GNPs. Therefore, the 20-cycle electrodeposition is recommended.

Figure 5 displays the effect of the amount of SOD on the cathodic response of the enzyme electrode. It can be seen that a maximum response occurs at concentration of SOD at 250 U mL^{-1} in the mixed sol solution. This is consistent with our previous report [16, 21]. Therefore, 250 U mL^{-1} SOD in the mixed solution was used for subsequent experiments.

Current–time response of the SOD–Cys–SG/GNPs/ITO electrode to superoxide anion

The amperometric response of the SOD–Cys–SG/GNPs/ITO electrode resulted from addition of superoxide anion is investigated in the stirred buffer solution at applied potential 210 mV. Superoxide anion was generated by addition of sodium hydroxide to dimethylsulphoxide (DMSO) [21, 24]. Briefly, the DMSO solution contained 5 mmol L^{-1} NaOH and 1% (v/v) H_2O was bubbled by air for about 3 min and then stabilized about 30 min. It can provide stable (at least 2 h), reproducible concentration of superoxide anion. The concentration of superoxide anion was obtained by UV spectrophotometry at 271 nm with the molar absorptivity (2,006 M^{-1} cm^{-1}) [24]. A peak-like response was observed because the concentration of superoxide anion decreased rapidly to the base level due to the dismutation in aqueous solution (Fig. 6), which is agreement with our previous reports [16, 21, 25].

Inset of Fig. 6 displays the calibration curve of the SOD–Cys–SG/GNPs/ITO electrode under the optimized experimental conditions. The linear range of superoxide anion is in the range of 0.08–0.64 μM with a correlation coefficient of 0.9937. The sensitivity of resulted biosensor is higher than that of SOD–SG/Au electrode [16] and SOD/GNPs/ITO electrode [20], but little lower than that of

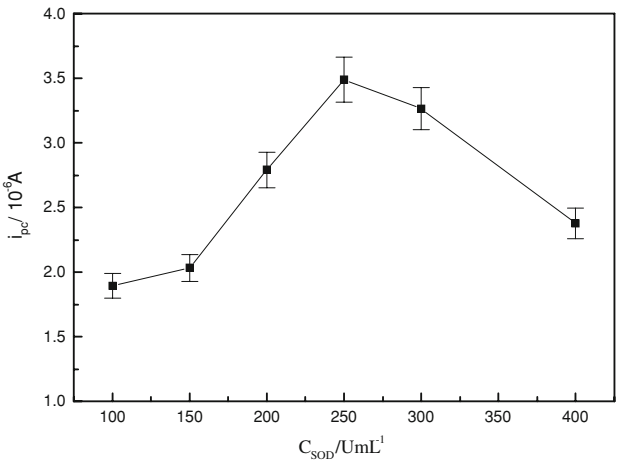

Fig. 5 Effect of the content of SOD for preparation of biosensor

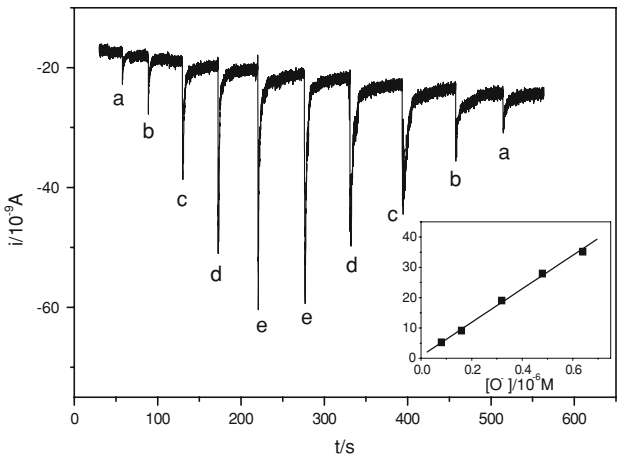

Fig. 6 Amperometric responses of SOD–Cys–SG/GNPs/ITO electrode to successive additions of superoxide anion-DMSO in 0.05 M PBS at applied potential of 0.210 V. Successive additions of superoxide anion-DMSO solution: *a* 0.08, *b* 0.16, *c* 0.32, *d* 0.48, *e* 0.64 μM. *Inset* is the linear calibration curve

SOD–GNP–Cys–SG/Au electrode [21]. A comparison to the works of Ohsaka and co-wokers [17–19] is difficult since they used a different calibration procedure.

The electrocatalytical activity towards superoxide anion was also investigated using the SOD–Cys–SG/GNPs/ITO electrode in which superoxide anion was generated from the classic reaction of xanthine oxidation by XOD. Figure 7 displayed typical amperometric responses towards successive addition of XOD in 1 μM xanthine and 0.05 M phosphate buffer solution. As can be readily seen from this figure, well-defined steady-state current responses increased linearly with superoxide anion concentrations (inset in Fig. 7). The amperometric response displays the "platform-like" because the concentration of superoxide anion is

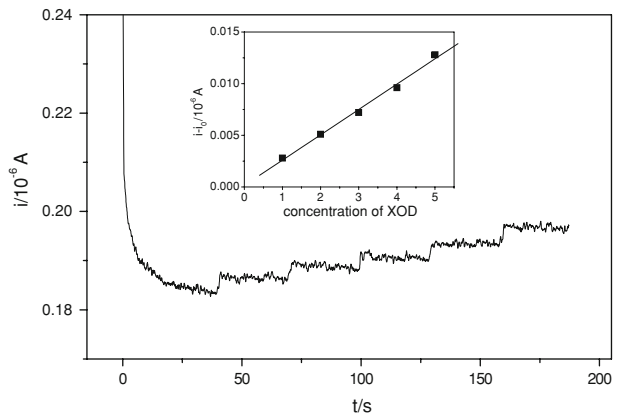

Fig. 7 Typical steady-state response of the SOD–Cys–SG/GNPs/ITO electrode on successive addition of 0.006 U mL^{-1} of XOD in 0.05 M^{-1} pH 7.0 PBS (O_2-saturated) containing 1 μM xanthine. Polarized potential, 0.21 V. *Inset* the calibration curve of the enzyme electrode

stable after addition of the aliquot XOD in this system. These results demonstrated that the proposed enzyme electrode has excellent responses to superoxide anion.

Reproducibility and stability of the disposable superoxide anion biosensor

The stability of the SOD–Cys–SG/GNPs/ITO electrode examined at a superoxide anion concentration of 0.2 μM, and the relative standard deviation was 3.7% ($n = 7$). The fabrication reproducibility was also investigated. The relative deviation was 6.4% at five different electrodes.

The storage stability of the superoxide anion biosensor was tested over a 90-day period. When the biosensor was stored in the refrigerator at 4 °C, it retained 85% of its initial current response after intermittent use over this period. This stability is much better than that of SOD/GNPs/ITO electrode [20], and the SOD electrode reported by Beissenhirtz and co-workers [26]. Good long-term stability can be due to the excellent biocompatible matrix for SOD immobilized on GNP surface in silica SG network.

Conclusions

The results clearly suggested that the strategy based on electrochemical deposition of GNPs on the ITO electrode as the substrate and then entrapment of SOD in silica SG network in the presence of cysteine is an effective route for fabrication of disposable superoxide anion biosensors. This matrix is very efficient for retaining the enzyme activity and preventing its leakage out of the network. The resulted biosensor possesses high sensitivity, good accuracy, and long-time stability. Moreover, it adopts low-cost ITO coated film glass as substrate and the construction techniques are suitable to large-area and large-scale industrial production. It is promising for fabrication of disposable biosensors in industrial production. This strategy further offers alternatives for construction of other disposable biosensors.

Acknowledgments This work was supported by the National Natural Science Foundation of China (No. 20675055) and the science foundations of the education bureau of Jiangsu Province (07KJB150101).

References

1. Afonso V, Champy R, Mitrovic D, Collin P (2007) Reactive oxygen species and superoxide dismutases: role in joint diseases. Joint Bone Spine 74:324–329
2. Auchère F, Rusnak F (2002) What is the ultimate fate of superoxide anion in vivo? J Biol Inorg Chem 7:664–667

3. Cepinskas G, Rui T, Kvietys PR (2002) Interaction between reactive oxygen metabolites and nitric oxide in oxidant tolerance. Free Radic Biol Med 33:433–440
4. Halliwell B, Gutteridge JMC (1984) Oxygen toxicity, oxygen radicals, transition metals and disease. Biochem J 219:1–14
5. Kehrer JP (2000) The Haber–Weiss reaction and mechanisms of toxicity. Toxicology 149:43–50
6. Seifried HE, Anderson DE, Fisher EI, Milner JA (2007) A review of the interaction among dietary antioxidants and reactive oxygen species. J Nutr Biochem 18:567–579
7. Ottaviani MF, Spallaci M, Cangiotti M, Bacchiocca M, NinfaliJ P (2001) Electron paramagnetic resonance investigations of free radicals in extra virgin olive oils. Agric Food Chem 49:3691–3696
8. Diez L, Livertoux M, Stark A, Wellman-Rousseau M, Leroy P (2001) High-performance liquid chromatographic assay of hydroxyl free radical using salicylic acid hydroxylation during in vitro experiments involving thiols. J Chromatogr B Analyt Technol Biomed Life Sci 763:185–193
9. Tsukagoshi K, Taniguchi T, Nakajima R (2007) Analysis of antioxidants using a capillary electrophoresis with chemiluminescence detection system. Anal Chim Acta 589:66–70
10. Yao D, Vlessidis AG, Gou Y, Zhou X, Zhou Y, Evmiridis NP (2004) Chemiluminescence detection of superoxide anion release and superoxide dismutase activity: modulation effect of *Pulsatilla chinensis*. Anal Bioanal Chem 379:171–177
11. Zhang L, Tang B, Ding Y (2005) Study of 2-(2-pyridyl)benzothiazoline as a novel fluorescent probe for the identification of superoxide anion radicals and the determination of superoxide dismutase activity in scallion genus foods. J Agric Food Chem 53:549–553
12. Tang B, Wang Y, Ma L (2004) Simple and rapid catalytic spectrophotometric determination of superoxide anion radical and superoxide dismutase activity in natural medical vegetables using phenol as the substrate for horseradish peroxidase. Anal Bioanal Chem 378:523–528
13. McNeil CJ, Manning P (2002) Sensor-based measurements of the role and interactions of free radicals in cellular systems. Rev Mol Biotechnol 82:443–455
14. Campanella L, Persi L, Tomassetti M (2000) A new tool for superoxide and nitric oxide radicals determination using suitable enzymatic sensors. Sens Actuators B 68:351–359
15. Lvovich V, Scheeline A (1997) Amperometric sensors for simultaneous superoxide and hydrogen peroxide detection. Anal Chem 69:454–462
16. Di J, Bi S, Zhang M (2004) Third-generation superoxide anion sensor based on superoxide dismutase directly immobilized by sol–gel thin film on gold electrode. Biosens Bioelectron 19:1479–1486
17. Tian Y, Mao L, Okajima T, Ohsaka T (2002) Superoxide dismutase-based third-generation biosensor for superoxide anion. Anal Chem 74:2428–2434
18. El-Deab MS, Ohsaka T (2007) Direct electron transfer of copper–zinc superoxide dismutase (SOD) on crystallographically oriented Au nanoparticles. Electrochem Commun 9:651–656
19. Tian Y, Mao L, Okajima T, Ohsaka T (2005) A carbon fiber microelectrode-based third-generation biosensor for superoxide anion. Biosens Bioelectron 21:557–564
20. Wang L, Mao W, Ni D, Di J, Wu Y, Tu Y (2008) Direct electrodeposition of gold nanoparticles onto indium/tin oxide film coated glass and its application for electrochemical biosensor. Electrochem Commun 10:673–676
21. Di J, Peng S, Shen C, Gao Y, Tu Y (2007) One-step method embedding superoxide dismutase and gold nanoparticles in silica sol–gel network in the presence of cysteine for construction of third-generation biosensor. Biosens Bioelectron 23:88–94
22. Dai X, Compton RG (2006) Direct electrodeposition of gold nanoparticles onto indium tin oxide film coated glass: application to the detection of arsenic (III). Anal Sci 22:567–570
23. Tian Y, Ariga T, Takashima N, Okajima T, Mao L, Ohsaka T (2004) Self-assembled monolayers suitable for electron-transfer promotion of copper, zinc-superoxide dismutase. Electrochem Commun 6:609–614
24. Choi MF, Hawkins P (1995) The contact charge transfer absorption spectrum of dimethysulphoxide with oxyen. Spectrochim Acta [A] 51:579–585
25. Lisdat F, Ge B, Ehrentreich-Förster E, Reszka R, Scheller FW (1999) Superoxide dismutase activity measurement using cytochrome *c*-modified electrode. Anal Chem 71:1359–1365
26. Beissenhirtz MK, Scheller FW, Viezzoli MS, Lisdat F (2006) Engineered superoxide dismutase monomers for superoxide biosensor applications. Anal Chem 78:928–935